Mass loss of Larsen B tributary glaciers (Antarctic Peninsula) unabated since 2002

Etienne Berthier, Ted A. Scambos, Christopher A. Shuman

Mass loss of Larsen B tributary glaciers (Antarctic Peninsula) unabated since 2002

Running Title:

Unabated mass loss in the Larsen B embayment

Etienne Berthier*, CNRS, Université de Toulouse, LEGOS, 14 av. Ed. Belin Toulouse 31400 France 33 5 61 33 29 66 etienne.berthier@legos.obs-mip.fr

Ted A. Scambos, NSIDC-CIRES, Campus Box 449, University of Colorado Boulder, CO 80309 USA; 1 303 492 1113 teds@nsidc.org

Christopher A. Shuman, UMBC-JCET, Code 615, NASA Goddard Space Flight Center Greenbelt, MD 20771 USA; 1 301 614 5706
christopher.a.shuman@nasa.gov

* corresponding author

Berthier E., Scambos T. A., and Shuman C. A. Mass loss of Larsen B tributary glaciers (Antarctic Peninsula) unabated since 2002, *Geophysical Research Letters*, 39, L13501, 10.1029/2012GL051755, 2012.

Abstract

Ice mass loss continues at a high rate among the large glacier tributaries of the Larsen B Ice Shelf following its disintegration in 2002. We evaluate recent mass loss by mapping elevation changes between 2006 and 2010/11 using differencing of digital elevation models (DEMs). The measurement accuracy of these elevation changes is confirmed by a 'null test', subtracting DEMs acquired within a few weeks. The overall 2006-2010/11 mass loss rate (9.0±2.1 Gt a^{-1}) is similar to the 2001/02-2006 rate (8.8±1.6 Gt a^{-1}), derived using DEM differencing and laser altimetry. This unchanged overall loss masks a varying pattern of thinning and ice loss for individual glacier basins. On Crane Glacier, the thinning pulse, initially greatest near the calving front, is now broadening and migrating upstream. The largest losses are now observed for the Hektoria/Green glacier basin, having increased by 33% since 2006. Our method has enabled us to resolve large residual uncertainties in the Larsen B sector and confirm its state of ongoing rapid mass loss.

1. Introduction

It is now well-demonstrated that the larger, deeper tributary glaciers of the Larsen A and B ice shelves have dramatically accelerated, retreated and thinned in response to the disintegration events of 1995 and 2002 [*De Angelis and Skvarca*, 2003; *Pritchard et al.*, 2009; *Rignot et al.*, 2004; *Rott et al.*, 2002; *Rott et al.*, 2011; *Scambos et al.*, 2004; *Shuman et al.*, 2011]. Although the collapse of a floating ice shelf has no direct impact on sea level, the increased ice discharge from grounded tributary glaciers does contribute significant mass to the ocean. However, there are still large and unexplained discrepancies (range: 4-22 Gt a^{-1}) between the ice losses inferred for the larger tributary glaciers that fed the Larsen B ice shelf (hereafter referred to as the northern Larsen B tributary glaciers, NLBTG, comprising the Hektoria-Green-Evans glacier system, Jorum and Punchbowl glaciers, Crane Glacier, and Mapple, Melville, and Pequod glaciers; see Figure 1) using different assessment methods [*Rignot et al.*, 2004; *Rott et al.*, 2011; *Shuman et al.*, 2011].

47 Nearly a decade after the ice shelf collapsed, reconciling estimates of the NLBTG mass imbalance
48 contribution is essential.

49 Three methods are presently available to measure the changes in the mass of an ice sheet, or a
50 portion of it: space gravimetry; the mass budget method (MBM); and the geodetic method (GM).
51 Space gravimetry from the Gravity Recovery and Climate Experiment (GRACE) is currently not
52 able to resolve mass losses occurring at a length scale of a few tens of kilometers, the typical size
53 of the NLBTG basins, and thus has been applied broadly to the Antarctic Peninsula north of 70°S
54 (Graham Land) where a steady decrease in mass is observed since 2002 (-32±6 Gt a^{-1} [*Ivins et al.*,
55 2011]; -28.6 Gt a^{-1} [*Chen et al.*, 2009]). The MBM consists of comparing the input (net
56 accumulation) to the output (ice flux through a cross-sectional gate at, or close to, the grounding
57 line). One determination using MBM for all basins between Hektoria and Crane glaciers (Figure
58 1), indicated mass losses of 21.9±6.6 Gt a^{-1} in 2003 [*Rignot et al.*, 2004] (30% uncertainty from
59 Rignot [2006]). Recently, the same technique was applied to the same glaciers by another group
60 using velocity fields measured in 2008/2009 in comparison with velocities from 1995-1999 [*Rott*
61 *et al.*, 2011]. Despite small changes in surface velocities since 2003 overall, they reported mass
62 losses of 4.1±1.6 Gt a^{-1}, a factor of 5 lower than the previous MBM study.

63 A geodetic estimate of the regional mass loss can be obtained by the differencing of digital
64 elevation models (DEMs) acquired a few years apart. Differencing of DEMs acquired prior to the
65 Larsen B ice shelf disintegration in November 2001 (extended to the upper part of Crane Glacier
66 with a DEM acquired in November 2002) with one acquired in November 2006, yields a distinctly
67 different estimate of the NLBTG mass loss, 8.8±1.6 Gt a^{-1} [*Shuman et al.*, 2011].

68 The causes of the differences between the three published NLBTG loss estimates are not
69 understood yet. Likely factors are (i) different time periods surveyed combined with non-steady
70 mass loss response, (ii) uncertainties in net accumulation for the MBM, (iii) unknown bed
71 topography close to the grounding line for most glaciers, (iv) unaccounted surface drawdown at

MBM flux gates, (v) errors in the DEMs for the GM; and (vi) grounding line migration for the GM and the MBM. Both the MBM estimates discussed above and our GM study use 900 kg/m^3 as density for converting volume to mass. Using this density (instead of that for pure ice, 917 kg/m^3) in the Larsen B sector is justified by the fact that the elevation changes are nearly entirely dynamically-driven, and that the entire column of ice (pure ice, firn, and snow) is being lost by calving at the ice fronts. By our estimate about 80% of the losses occur on fast flowing glacier trunks below 500 m a.s.l.

In this study, we use new 2010 and 2011 satellite DEMs to infer the mass loss of NLBTG between 2006 and 2010/11. These updated mass losses are then compared to 2001/02-2006 losses to determine how NLBTG losses have evolved over time since the break up and, thus, to partly address issue (i). In addition, satellite DEMs acquired within a few weeks in late 2006 are compared to better constrain the uncertainties associated with the GM (issue v). A basin-by-basin comparison is also performed to identify the glaciers for which the discrepancies between MBM and GM estimates are largest and help to target future data acquisition to reconcile estimates of the NLBTG mass imbalance (issue iii). Our elevation changes time series from DEMs (augmented with airborne and satellite laser altimetry) helps to address issue (iv). Grounding line migration since 2002 has probably been rapid, with the ice fronts quickly retreating past its 1990s position [*Shuman et al.,* 2011]. Satellite imagery suggests the present ice fronts are partially floating, complicating flux gate assessments [*Zgur et al.*, 2007; *Rott et al.*, 2011].

2. Data Sets and Methods

Our analysis is based on seven DEMs of the NLBTG derived from ASTER [*Fujisada et al.*, 2005] and SPOT5 [*Korona et al.*, 2009] optical stereo-imagery (Table S1, Figure S1 and S2). The processing steps followed to horizontally/vertically adjust the DEMs have been described in detail previously [e.g., *Shuman et al.*, 2011] and are briefly summarized here. Cloudy and unreliable

pixels are masked. All DEMs are first horizontally co-registered to the reference DEM (the 25 November 2006 SPOT5 DEM) by minimizing the standard deviation of the elevation differences. Then, all DEMs are vertically adjusted to the 25 November 2006 DEM using the (assumed) stable regions outside of the fast changing outlet glaciers. Only a constant vertical offset is corrected for each DEM around each major basin (the average of the vertical bias within each basin, typically less than 5 m), neglecting any spatial variations in the vertical bias within each basin.

3. Null tests: accuracy of the mass loss from sequential DEMs

We analyze three DEMs acquired within a short time span in late 2006 (Table S1) to assess the accuracy of the ASTER/SPOT5 and SPOT5/SPOT5 basin-wide elevation changes. The assumption of insignificant elevation change is valid between the SPOT5 and ASTER DEMs as they were acquired only 16 minutes apart on 25 November 2006. This assumption is not as appropriate between the 25 November 2006 and the 31 December 2006 SPOT5 DEMs, with 36 days elapsed. The rates of elevation changes measured during 2001/02-2006 [*Shuman et al.*, 2011, their Table 2] are used to estimate 36-day elevation changes within each major basin. Based on this, the maximum change is -0.7 m for Evans Glacier and the smallest is for Jorum Glacier at –0.2 m. Basin-wide mean DEM differences (Table 1) provide null test errors for the GM applied to the NLBTG.

For individual drainage basins, the errors are larger for ASTER/SPOT5 than for SPOT5/SPOT5. This is expected given the higher image resolution and the better orbit knowledge for the SPOT5 sensor so that SPOT5 DEMs are about a factor of two more precise than ASTER DEMs [*Berthier et al.*, 2010, their Table S5]. The basin-wide elevation difference in the ASTER/SPOT5 comparison reaches 5.0 m for Crane Glacier. This result confirms the ±5 m elevation error used previously [*Shuman et al.*, 2011]. In contrast, the basin-wide elevation difference is always less than 2 m for SPOT5/SPOT5 differences. When the mean elevation

122 difference is computed for all NLBTG basins, errors are 2.4 m for ASTER/SPOT5 and 1.0 m for
123 SPOT5/SPOT5.
124 In the following assessments of volume and mass change, a ±2 m (respectively, ±5 m)
125 uncertainty is used when two SPOT5 (respectively, ASTER and SPOT5) DEMs are subtracted.
126 Our null tests indicate that these uncertainties are reasonable at the individual basin scale, and are
127 conservative for elevation differences averaged over all NLBTG.
128
129 **4. Elevation changes and mass loss in 2006-2010/11**
130 Recent elevation changes for NLBTG are measured by subtracting two SPOT5 DEMs (31
131 December 2006 and 14 March 2011) for a 2633 km² area in the west and a SPOT5 (25 November
132 2006) DEM and an ASTER (15 December 2010) DEM for a 906 km² area in the east (Figure 1).
133 The rates of elevation changes during 2006-2010/11 are compared to those reported in *Shuman et*
134 *al.* [2011] during 2001/02-2006 (Figures 2 and 3, Table 2).
135 Between the two epochs, the maximum mean annual thinning rate considerably diminished for
136 Crane Glacier from over 35 m a^{-1} to 18 m a^{-1}. We note that the peak elevation loss during 2001/02-
137 2006 was likely influenced by a sub-glacial lake drainage event that occurred between September
138 2004 and September 2005 in the lower Crane Glacier [*Scambos et al.*, 2011], but a region of >20 m
139 a^{-1} loss extended over a far larger area than the inferred lake extent in the lower glacier trunk.
140 During 2006-2010/11, thinning has propagated further upstream, and the 10 m a^{-1} thinning rate
141 contour has moved from 500 m a.s.l. to 700 m a.s.l between the two assessments. An upstream
142 migration of thinning is also observed for Hektoria and Green glaciers with the upper extent of the
143 10 m a^{-1} thinning contour moving from 350 to 500 m a.s.l. between the two epochs. For the latter
144 two glaciers, the peak thinning rates are higher during 2006-2010/11 (35 m a^{-1}) than during
145 2001/02-2006 (23 m a^{-1}). For the main trunks of Hektoria, Green and Crane glaciers, the horizontal
146 speed of inland propagation of the 10 m a^{-1} thinning contour is similar, at about 2 km a^{-1}.

147 Total mass losses from Hektoria and Green glaciers have increased by one third since the
148 earlier period (from 4.2 to 5.6 Gt a^{-1}). Their ice front positions have also varied considerably since
149 2002, with both retreats and advances [*Shuman et al.*, 2011]. This makes these glaciers the main
150 contributors to the regional losses (Table 2), ahead of Crane Glacier where net mass loss and ice
151 front position (since ~2006) have remained nearly unchanged.
152 South of the major NLBTG glaciers, elevation changes of Mapple, Melville and Pequod
153 glaciers are small despite the fact that they have been less constrained since the Larsen B ice shelf
154 disintegration. In our earlier study, we noted that these glaciers have shallower seabed bathymetric
155 troughs in front of them, and likely had less of their longitudinal resistive stresses derived from the
156 former ice shelf [*Shuman et al.*, 2011; *Zgur et al.*, 2007].
157

158 **5. Discussion**

159 The null test in Section 3 demonstrates that for all NLBTG (~3000 km²), area-average
160 elevation changes can be measured with an accuracy of ±1 m (using two SPOT5 DEMs) and ±2.5
161 m (using one ASTER and one SPOT5 DEM). These null test errors can be compared to the
162 standard errors, often applied in differential DEMs studies [e.g., *Nuth and Kääb*, 2011]. The
163 standard errors are computed from the standard deviation of the DEMs (typically ±10 m for
164 SPOT5 and ±15 m for ASTER) after accounting for the number of independent samples. For all
165 NLBTG basins, and assuming autocorrelation lengths of 200 m [*Howat et al.*, 2008] / 500 m
166 [*Berthier et al.*, 2010] / 1000 m [*Nuth et al.*, 2007], standard error of, respectively ±0.7 m / ±1 m /
167 ±1.5 m are derived for the ASTER/SPOT5 comparison. Those standard errors are all lower than
168 our null test error (±2.5 m), probably due to spatially-varying vertical biases in the DEMs [*Nuth*
169 *and Kääb*, 2011] that cannot be accounted for by a single shift measured on (assumed) stable
170 regions. Modeling these complex vertical biases in the DEMs using ICESat laser altimetry data
171 was attempted. This is not discussed here because ICESat data are too scarce in our study region to

172 further refine the error bars calculated in the null test. Such a strategy of DEM adjustment using
173 precise external data would be certainly useful in glaciated areas where stable ground is effectively
174 absent, where the density of altimetry data is higher (e.g., closer to 86° latitude for ICESat) and
175 where the altimetry surveys are performed close-in-time to the DEMs.

176 Geodetic mass losses upstream of the pre-collapse grounding line [*Rack and Rott*, 2004] are
177 virtually unchanged since 2002 for the grounded NLBTG (8.8±1.6 Gt a^{-1} for 2001/02-2006 and
178 9.0±2.1 Gt a^{-1} for 2006-2010/11, Table 2). This finding is in agreement with limited changes in
179 velocities for most glaciers between 2003 and 2008/2009 [*Rott et al.*, 2011], despite some shorter
180 term flow variability for Crane [*Rignot*, 2006; *Scambos et al.*, 2011] and Hektoria [*Rignot*, 2006;
181 *Rott et al.*, 2011] glaciers. The consistency of the mass loss through time between 2002 and
182 2010/11 is also independently supported by the regional GRACE time series [*Ivins et al.*, 2011]
183 and by a continuous elastic uplift of the solid earth since 2002 at the Palmer GPS station, ~100 km
184 west of NLBTG [*Thomas et al.*, 2011]. Our analyses reveal an evolving pattern of elevation
185 changes, with a wave of glacier thinning that has broadened and migrated rapidly upstream over
186 time.

187 Our GM mass loss estimates for NLBTG lie between the losses inferred by the two earlier
188 studies using the MBM, suggesting that losses are overestimated by 12.9±6.9 Gt a^{-1} in *Rignot et al.*
189 [2004] and underestimated by 4.7±2.6 Gt a^{-1} in *Rott et al.* [2011]. Quantifying and understanding
190 these large discrepancies is important because these methods (MBM and GM) are employed to
191 determine the mass balance of glaciers in the Peninsula, a region which alone contribute about one
192 fourth of the continent-wide mass imbalance [e.g., *Rignot et al.*, 2008]. It is also crucial to provide
193 realistic scenarios of mass losses following ice shelf collapse to test the ability of ice flow models
194 to simulate them. We note that the GM method requires far fewer assumptions than the MBM in
195 the Larsen B region, with well-constrained differential DEM errors (section 3). Both bed
196 topography and surface mass balance are poorly known for the NLBTG. For Crane Glacier only,

197 bed topography at the present grounding line can be inferred by extrapolating upstream bathymetry
198 data collected in 2006 [*Rott et al.*, 2011; *Zgur et al.*, 2007]. The authors of the preceding MBM-
199 based studies had, by necessity, to assume the glaciers to be in equilibrium before the Larsen B ice
200 shelf collapse and computed the pre-collapse ice discharge from a model estimate of net
201 accumulation over the catchment basins. However, recent assessments of surface mass balance
202 (net accumulation) for Antarctica [*Lenaerts et al.*, 2012], and a review of some field measurements
203 for the region reported in *Rott et al.* [2011], as well as field evidence from ongoing monitoring by
204 one of us (TAS) indicate that the effective net accumulation (~1900 kg m^{-2} a^{-1}) used by *Rignot et*
205 *al.* [2004] was too large. A strong accumulation gradient exists across the NLBTG area, with
206 progressively decreasing snow input east of the Antarctic Peninsula divide. Measured
207 accumulation rates as part of an ongoing study (LARISSA: Larsen Ice Shelf System Antarctica)
208 reach 2000 to 3000 kg m^{-2} a^{-1} at the divide [*Zagorodnov et al.*, in press], but are < 300 kg m^{-2} a^{-1}
209 near 450 m a.s.l. on the nearby Flask and Leppard glacier outlets. Applying the basin-wide mean
210 net accumulation value indicated by *Rott et al.* [2011], 1087 kg m a^{-1}, would adjust the mass
211 imbalance reported by *Rignot et al.* [2004] to 57% of the value reported, or ~12.2 Gt a^{-1} for the
212 NLBTG region (if the accumulation correction ratio holds for the entire area).

213 We partially reconcile our net imbalance estimate on Crane Glacier with the value reported by
214 *Rott et al.* [2011] by considering the velocity variations observed over the past decade [*Scambos et*
215 *al.*, 2011]. A sequence of visible and near-infrared satellite images shows more than one
216 acceleration period, and in particular ice flow speed in late 2006 was 1.3 times the level in late
217 2008 (the time of the *Rott et al.* measurement). Further slowing occurred on Crane Glacier between
218 2008 and 2009 [*Rott et al.*, 2011; *Scambos et al.*, 2011]. Thus, our geodetic method, which
219 integrates over a 5-year period, may be expected to show a higher value than a shorter-term
220 assessment during a single period of slower flow speed.

During the two epochs studied here, Hektoria and Green glaciers have been the major contributors to the regional mass loss (over 60% of total loss during 2006-2010/11). This is also where the largest discrepancies in the MBM estimates are observed in our study area. The data most needed to reconcile estimates of the mass loss in the Larsen B embayment are bed topography profiles from ice-penetrating radars for the Hektoria and Green glaciers.

6. Conclusion

At 8.9 Gt a^{-1}, our 2002-2011 NLBTG mass loss estimate represents about one third of the overall loss observed with GRACE in the Graham Land of the Antarctic Peninsula [*Chen et al.*, 2009; *Ivins et al.*, 2011]. An implication is that rapid ice loss and surface lowering are occurring elsewhere in the northern Antarctic Peninsula as indicated by other studies [*Glasser et al.*, 2011; *Pritchard and Vaughan*, 2007; *Pritchard et al.*, 2009]. Our results suggest that differential DEM analysis would provide similar insights on the mass balance for all of Graham Land and similar glaciated regions with mostly unknown ice thickness and spatially varying surface mass balance.

We have re-assessed the glaciers of the Larsen B embayment where variations in published mass balance assessments are largest (up to 300%) and suggest that poorly constrained bedrock topography and net accumulation are the reasons for this range, primarily affecting the MBM method. Our differential DEM analysis shows continuing steady net losses from the Larsen B embayment glaciers overall but with accelerating losses for the northern Hektoria/Green basin.

7. Acknowledgements

We thank G. Durand, B. Kulessa and four anonymous referees for their comments on earlier versions of the manuscript. EB acknowledges support from CNES (TOSCA and ISIS proposals), PNTS, and ANR-09-SYSC-001. TAS acknowledges support from NSF-OPP, ANT-0732921, and NASA NNX10AR76G grants. CAS was supported by grants from the NASA Cryospheric

Sciences Program. SPOT5 HRS data were provided at no cost by CNES through the SPIRIT project. ASTER data were provided at no cost by NASA/USGS through the Global Land Ice Measurements from Space (GLIMS) project.

8. References

Berthier, E., E. Schiefer, G. K. C. Clarke, B. Menounos, and F. Remy (2010), Contribution of Alaskan glaciers to sea-level rise derived from satellite imagery, *Nat Geosci*, *3*(2), 92-95.

Chen, J. L., C. R. Wilson, D. Blankenship, and B. D. Tapley (2009), Accelerated Antarctic ice loss from satellite gravity measurements, *Nat Geosci*, *2*(12), 859-862.

De Angelis, H., and P. Skvarca (2003), Glacier Surge After Ice Shelf Collapse, *Science*, *299*(5612), 1560-1562.

Fujisada, H., G. B. Bailey, G. G. Kelly, S. Hara, and M. J. Abrams (2005), ASTER DEM performance, *IEEE T Geosci Remote*, *43*(12), 2707-2714.

Glasser, N. F., T. A. Scambos, J. Bohlander, M. Truffer, E. Pettit, and B. J. Davies (2011), From ice-shelf tributary to tidewater glacier: continued rapid recession, acceleration and thinning of Rohss Glacier following the 1995 collapse of the Prince Gustav Ice Shelf, Antarctic Peninsula, *J Glaciol*, *57*(203), 397-406.

Howat, I. M., B. E. Smith, I. Joughin, and T. A. Scambos (2008), Rates of southeast Greenland ice volume loss from combined ICESat and ASTER observations, *Geophys Res Lett*, *35*(17).

Ivins, E. R., M. M. Watkins, D.-N. Yuan, R. Dietrich, G. Casassa, and A. Rülke (2011), On-land ice loss and glacial isostatic adjustment at the Drake Passage: 2003–2009, *J Geophys Res-Earth*, *116*, B02403.

Korona, J., E. Berthier, M. Bernard, F. Remy, and E. Thouvenot (2009), SPIRIT. SPOT 5 stereoscopic survey of Polar Ice: Reference Images and Topographies during the fourth International Polar Year (2007-2009), *ISPRS J Photogramm*, *64*, 204-212.

Lenaerts, J. T. M., M. R. van den Broeke, W. J. van de Berg, E. van Meijgaard, and P. K. Munneke (2012), A new, high-resolution surface mass balance map of Antarctica (1979-2010) based on regional atmospheric climate modeling, *Geophys Res Lett*, *39*(L04501), 4501-4501.

Nuth, C., and A. Kääb (2011), Co-registration and bias corrections of satellite elevation data sets for quantifying glacier thickness change, *Cryosphere*, *5*(1), 271-290.

Nuth, C., J. Kohler, H. F. Aas, O. Brandt, and J. O. Hagen (2007), Glacier geometry and elevation changes on Svalbard (1936-90): a baseline dataset, *Ann Glaciol*, *46*, 106-116.

Pritchard, H. D., and D. G. Vaughan (2007), Widespread acceleration of tidewater glaciers on the Antarctic Peninsula, *J Geophys Res-Earth*, *112*(F3), F03S29.

Pritchard, H. D., R. J. Arthern, D. G. Vaughan, and L. A. Edwards (2009), Extensive dynamic thinning on the margins of the Greenland and Antarctic ice sheets, *Nature*, *461*(7266), 971-975.

Rack, W., and H. Rott (2004), Pattern of retreat and disintegration of the Larsen B ice shelf, Antarctic Peninsula, *Ann Glaciol*, *39*, 505-510.

Rignot, E. (2006), Changes in ice dynamics and mass balance of the Antarctic ice sheet, *Phil Trans R Soc A*, *364*(1844), 1637-1655.

Rignot, E., G. Casassa, P. Gogineni, W. Krabill, A. Rivera, and R. Thomas (2004), Accelerated ice discharge from the Antarctic Peninsula following the collapse of Larsen B ice shelf, *Geophys Res Lett*, *31*(18).

Rignot, E., J. L. Bamber, M. R. Van Den Broeke, C. Davis, Y. H. Li, W. J. Van De Berg, and E. Van Meijgaard (2008), Recent Antarctic ice mass loss from radar interferometry and regional climate modelling, *Nat Geosci*, *1*(2), 106-110.

Rott, H., W. Rack, P. Skvarca, and H. De Angelis (2002), Northern Larsen Ice Shelf, Antarctica: further retreat after collapse, *Ann Glaciol*, *34*, 277-282.

Rott, H., F. Müller, T. Nagler, and D. Floricioiu (2011), The imbalance of glaciers after disintegration of Larsen B ice shelf, Antarctic Peninsula, *Cryosphere*, *5*(1), 125-134.

296 Scambos, T. A., E. Berthier, and C. A. Shuman (2011), The triggering of sub-glacial lake drainage
297 during the rapid glacier drawdown: Crane Glacier, Antarctic Peninsula, *Ann Glaciol*, *52*(59), 74–
298 82.
299 Scambos, T. A., J. A. Bohlander, C. A. Shuman, and P. Skvarca (2004), Glacier acceleration and
300 thinning after ice shelf collapse in the Larsen B embayment, Antarctica, *Geophys Res Lett*, *31*(18),
301 L18402.
302 Shuman, C. A., E. Berthier, and T. A. Scambos (2011), 2001-2009 elevation and mass losses in the
303 Larsen A and B embayments, Antarctic Peninsula, *J Glaciol*, *57*(204), 737–754.
304 Thomas, I. D., et al. (2011), Widespread low rates of Antarctic glacial isostatic adjustment
305 revealed by GPS observations, *Geophys Res Lett*, *38*(L22302).
306 Zagorodnov, V., O. Nagornov, T. A. Scambos, A. Muto, E. Mosley-Thompson, E. C. Pettit, and T.
307 S. (in press), Borehole temperatures reveal details of 20th century warming at Bruce Plateau,
308 Antarctic Peninsula, *Cryosphere*.
309 Zgur, F., M. Rebesco, E. W. Domack, A. Leventer, S. Brachfeld, and V. Willmott (2007),
310 Geophysical survey of the thick, expanded sedimentary fill of the new-born Crane fjord (former
311 Larsen B Ice Shelf, Antarctica), *US Geological Survey and the National Academies; USGS OF-*
312 *2007-1047*, *Extended Abstract 141*.
313
314

315 **Tables**

316 Table 1. Basin-wide mean elevation differences (m) between DEMs acquired the same day (25
317 Nov. 2006, ASTER/SPOT5) and 36-days apart (SPOT5 25 Nov./SPOT5 31 Dec.). In bold, the
318 maximum absolute error for each method. The last row shows the mean differences for the entire
319 study region. MMP stands for the Mapple, Melville, and Pequod glaciers.
320

	ASTER/SPOT5	SPOT5/SPOT5*
Hektoria-Green	-3.0	-0.6
Evans	2.5	-1.2
Punchbowl-Jorum	-2.5	**-1.5**
Crane	**-5.0**	-1.4
MMP	2.0	-0.1
All NLBTG	-2.4	-1.0

321 * The 36-day elevation difference has been estimated and corrected using the 2001/02-2006
322 elevation change rate.
323
324
325 Table 2: Basin-by-basin mass changes (Gt a^{-1}) from different studies in the Larsen B embayment.

Reference	Rignot et al., 2004	Rott et al., 2011	Shuman et al., 2011	This Study
Method	Mass Budget	Mass Budget	Geodetic	Geodetic
Year / Epoch	2003	2008	2001/02-2006*	2006-2010/11
Hektoria-Green	-16.7±5.0	-1.7±0.6	-4.2±0.7	-5.6±0.8
Evans		-0.3±0.1	-1.7±0.3	-0.8±0.2***
Punchbowl-Jorum	-1.5±0.5	-0.3±0.2	-0.6±0.3	-0.4±0.3
Crane	-3.8±1.1	-1.8±0.6	-2.3±0.3	-2.4±0.5
MMP	-	-0.2±0.1	-	0.2±0.3
All Glaciers	**-21.9**±6.6	**-4.3**±1.6	**-8.8**±1.6**	**-9.0**±2.1

326 * Numbers slightly differ from [*Shuman et al.*, 2011] because here ice losses are assumed to entirely occur
327 after the March 2002 break-up. Areas of grounded ice that calved are not added to the total to enable
328 appropriate comparison to the MBM.
329 ** The lower uncertainties in 2001/02-2006 (compared to 2006-2010/11) are due to a smaller area
330 surveyed: only regions below 1000 m a.s.l. are considered. Exclusion of regions at high elevations is
331 justified by their lack of significant elevation changes in the earlier period [*Shuman et al.*, 2011].
332 *** This large decrease in mass loss after 2006 is uncertain because the lower part of Evans Glacier was
333 poorly sampled during 2006-2010/11.

334 **Figures**

335

336

337 Figure 1. Study area and the main drainage basins of the northern Larsen B embayment. All
338 glaciers studied here flowed into the Larsen B ice shelf before its collapse in 2002. Southern
339 tributaries (e.g., Flask and Leppard glaciers) still constrained by a remnant of the Larsen B ice
340 shelf are not considered. The area shaded in light blue is where elevation changes are measured
341 during 2006-2011; the area shaded in yellow has difference measurements during 2006-2010.
342 Background: Mosaic of 25 November 2006 and 31 December 2006 SPOT5 images (© CNES
343 2006, Spot Image). Inset: location of the study area in the north of the Antarctic Peninsula.

344

345 Figure 2. Rate of ice elevation changes (m a^{-1}) between 2001/02-2006 (left) and 2006-2010/11
346 (right). The 10 m a^{-1} thinning contour is shown with a gray dotted line, the 20 m a^{-1} with a dark
347 dotted line.

348

349 Figure 3. Rate of elevation change averaged for 50-m altitude bands for Crane (a) and
350 Hektoria/Green (b) during 2001/02-2006 (filled symbols) and 2006-2010/11 (unfilled symbols).
351 For clarity, errors bars are only shown in the legends. Insets are 3D surface views showing the
352 glaciers in 25 November 2006 (Copyright CNES 2006, Spot Image).

353

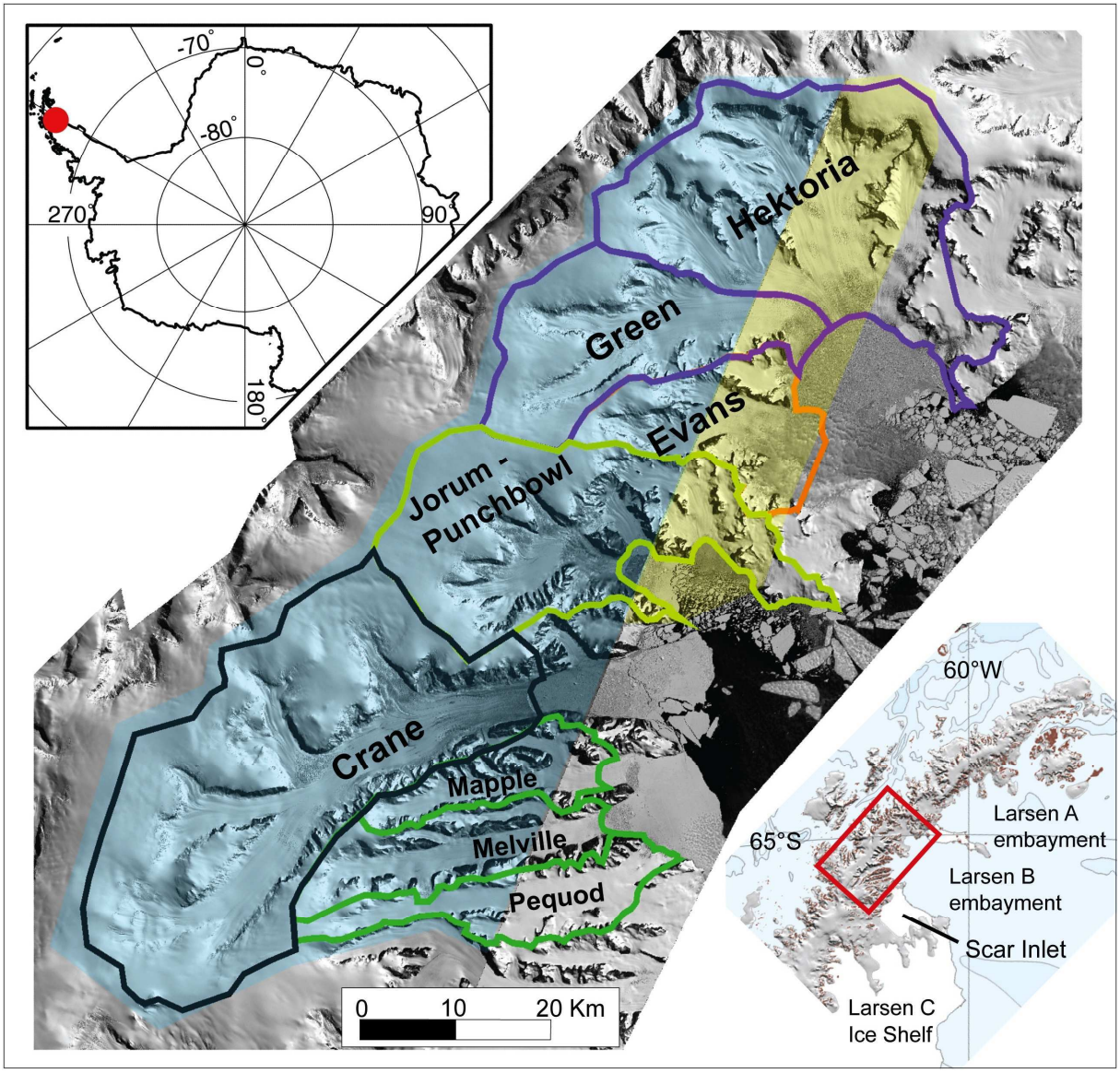
-70°
0°
-80°
270°
90°
180°
Hektoria
Green
Evans
Jorum -
Punchbowl
Crane
Mapple
Melville
Pequod
0
10
20 Km
60°W
65°S
Larsen A
embayment
Larsen B
embayment
Scar Inlet
Larsen C
Ice Shelf

354

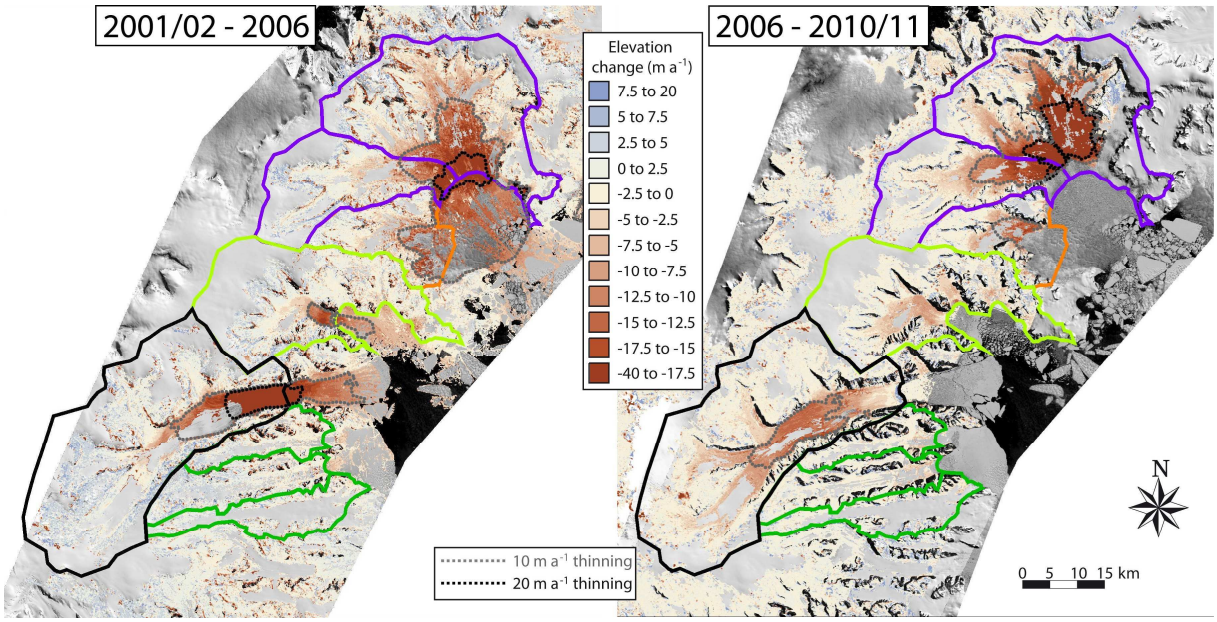
2001/02 - 2006
2006 - 2010/11
Elevation change (m a-1)
7.5 to 20
5 to 7.5
2.5 to 5
0 to 2.5
-2.5 to 0
-5 to -2.5
-7.5 to -5
-10 to -7.5
-12.5 to -10
-15 to -12.5
-17.5 to -15
-40 to -17.5
10 m a-1 thinning
20 m a-1 thinning
N
0 5 10 15 km

355

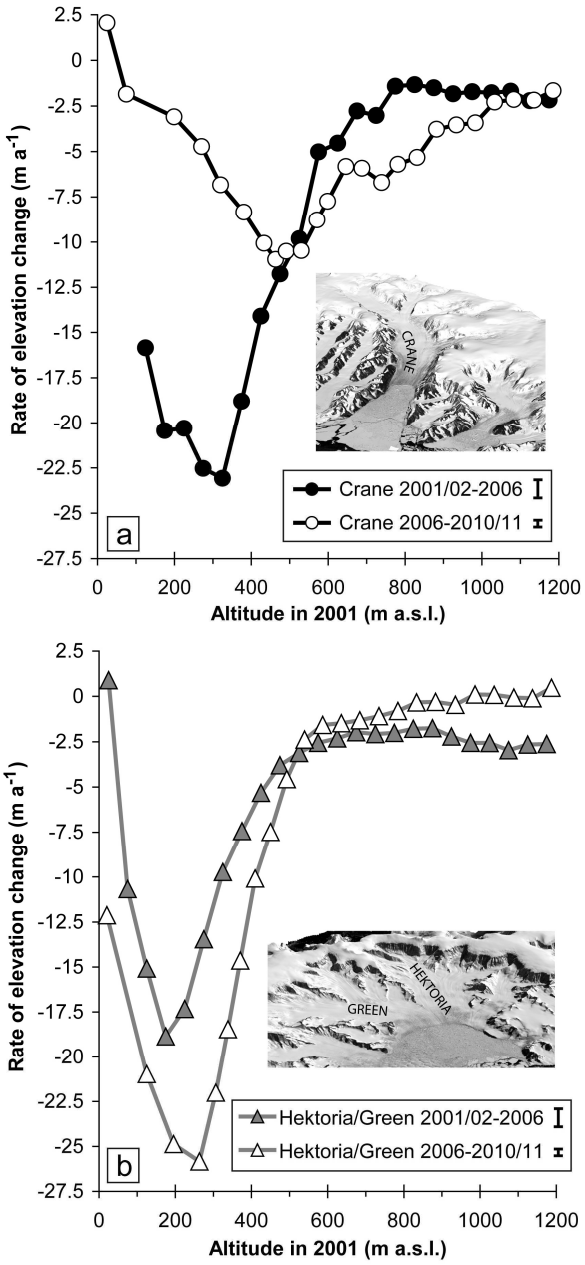
Rate of elevation change (m a-1)
2.5
0
-2.5
-5
-7.5
-10
-12.5
-15
-17.5
-20
-22.5
-25
-27.5
0
200
400
600
800
1000
1200
Altitude in 2001 (m a.s.l.)
a
CRANE
Crane 2001/02-2006
Crane 2006-2010/11
b
HEKTORIA
GREEN
Hektoria/Green 2001/02-2006
Hektoria/Green 2006-2010/11

356